Supporting Information

Tunable dielectric transitions in layered organic-inorganic hybrid perovskite-type compounds: $[NH_3(CH_2)_2Cl]_2[CdCl_{4-4x}Br_{4x}]$ (x=0, 1/4, 1)

Hai-Peng Chen, Ping-Ping Shi*, Zhong-Xia Wang, Ji-Xing Gao, Wan-Ying Zhang, Cheng Chen, Yuan-Yuan Tang and Da-Wei Fu*

Ordered Matter Science Research Center, Jiangsu Key Laboratory for Science and Applications of Molecular Ferroelectrics, Southeast University, Nanjing 211189, PR China

*E-mail: ppshi@seu.edu.cn, dawei@seu.edu.cn.

During the growth of the crystals of **1**, there may be a small difference in the amounts of doped halogen due to the subtle distinction between them. Not only that, the different growth times of those crystals will also be responsible for this. Therefore, for **1**, the experimental result of elemental analysis is acceptable and reasonable.

For crystal structures of **2**, the disorder degree of the cations is so high that the hydrogen atoms are unable to be added.

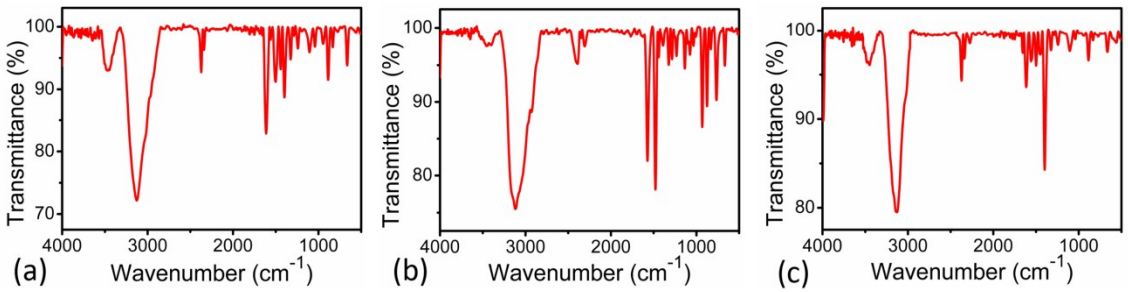

Fig. S1 Infrared (IR) spectra of **1** (a), **2** (b) and **3** (c) in KBr pellet recorded on a Shimadzu model IR-60 spectrometer at 293 K.

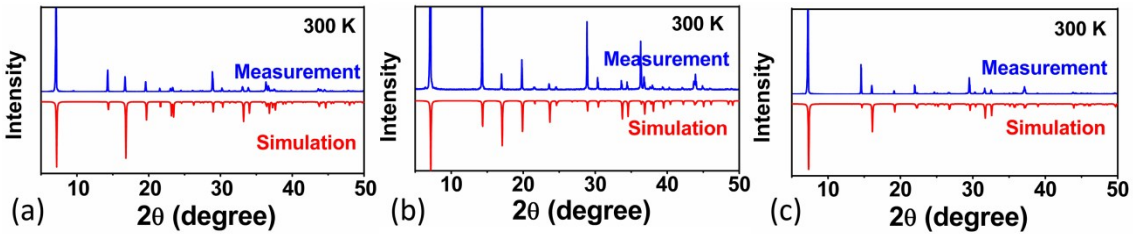

Fig. S2 Experimental powder X-ray diffraction patterns of **1** (a), **2** (b) and **3** (c) match very well with the simulated ones based on the crystal structures at 300 K.

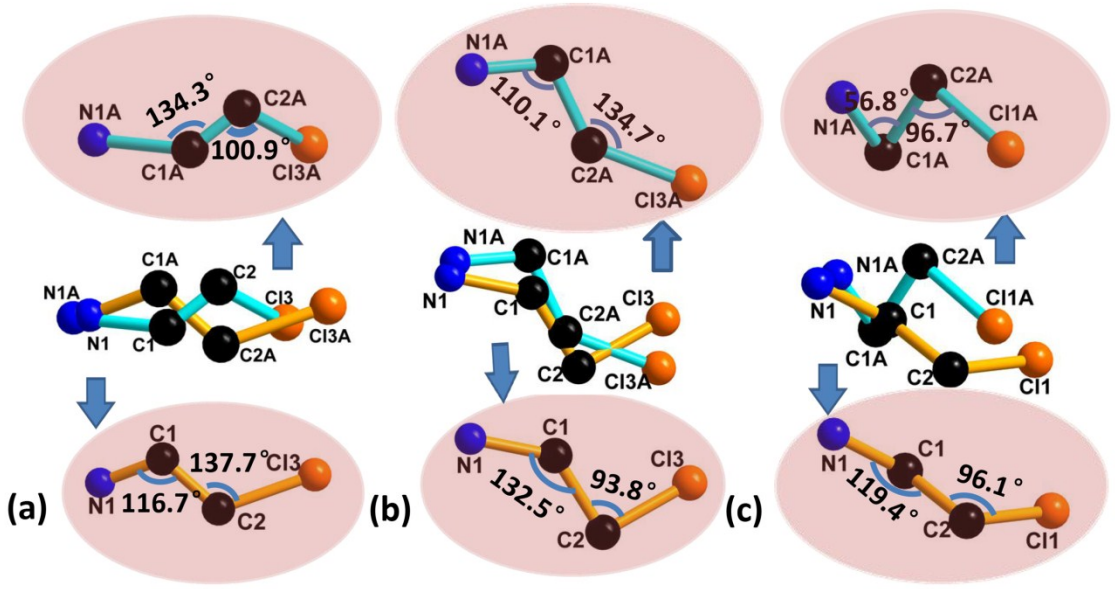

Fig. S3 Comparison of the bond angles of 2-chloroethanamine cations of **1** (a), **2** (b) and **3** (c) at 293 K. All hydrogen atoms were omitted for clarity.

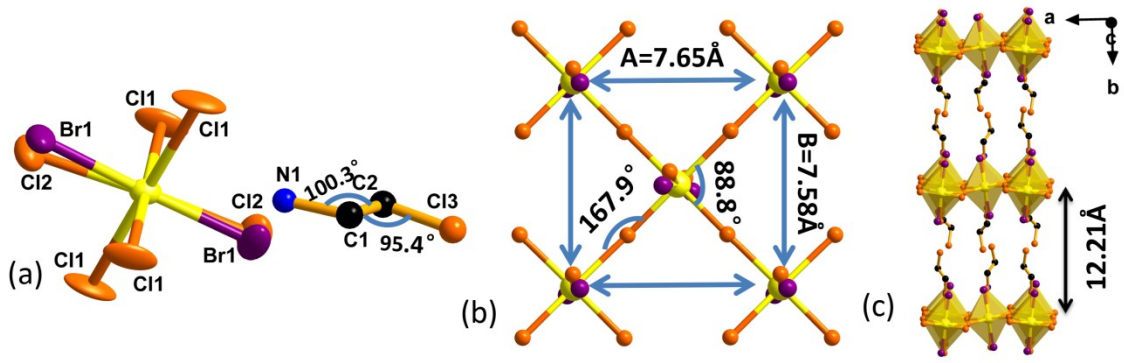

Fig. S4 (a) The molecular structure of **1** at 143 K. Thermal ellipsoids for all atoms of anion were shown at the 50% probability level. (b) The bond angle and Cd....Cd distances of anions of **1** at 143 K. (c) The packing diagram of **1** at 143 K, where $[ClC_2H_4NH_3]^+$ cations are located in the cavities between the layers. Hydrogen atoms are omitted for clarity.

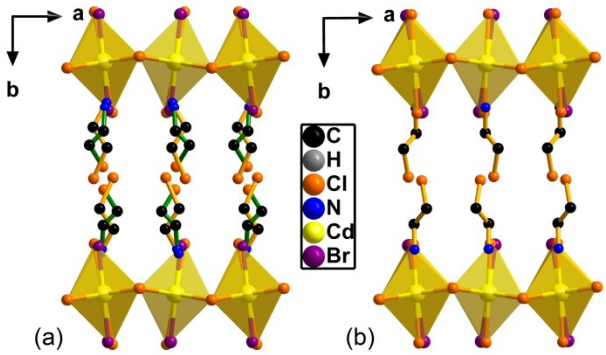

Fig. S5 Packing diagrams of **1** (a) at 293 K and (b) at 143 K, where $[ClC_2H_4NH_3]^+$ cations are located in the cavities between the layers. All hydrogen atoms were omitted for clarity.

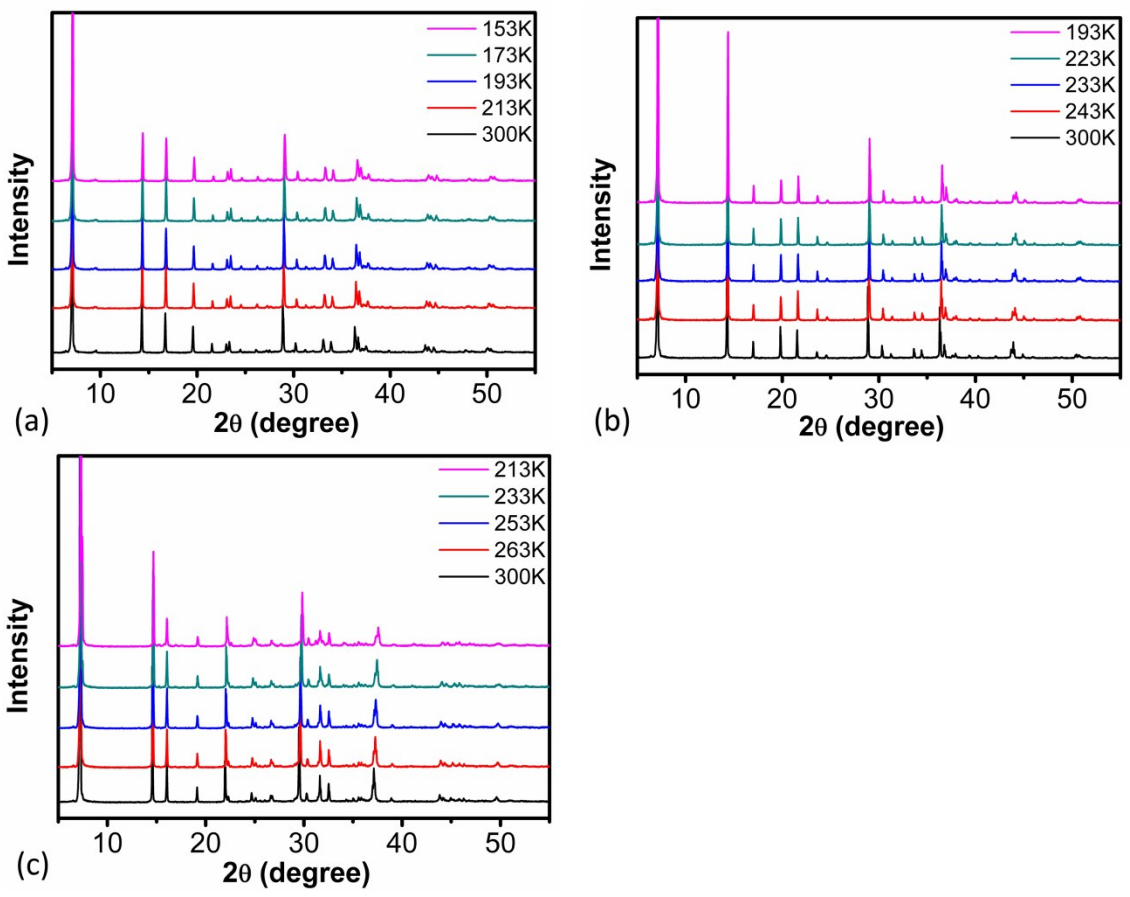

Fig. S6 Variable-temperature powder X-ray diffraction patterns of **1** (a), **2** (b) and **3** (c).

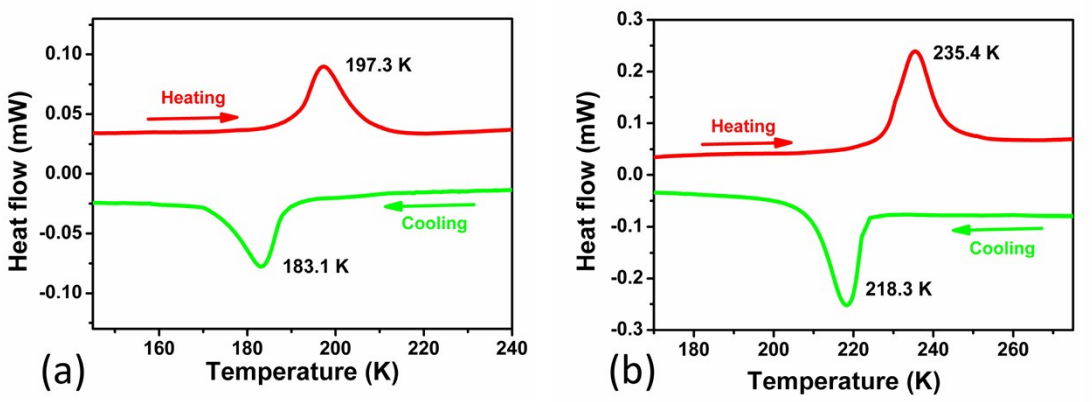

Fig. S7 DSC curves of **4** (a)) and **5** (b) obtained in the cooling and heating cycles.

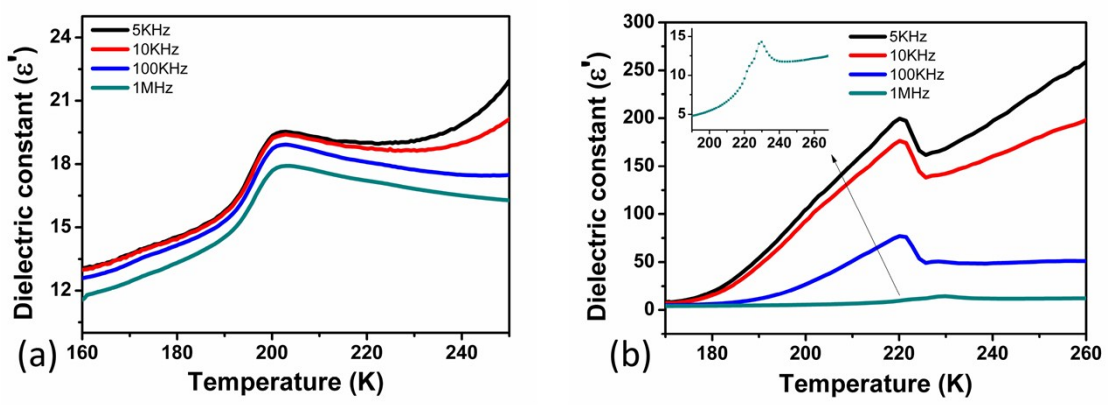

Fig. S8 The temperature-dependent dielectric constant (ε') of the polycrystalline samples of **4** (a) and **5** (b) measured at selected frequencies of 5 KHz, 10 KHz, 100 KHz and 1 MHz.

By applying the DSC and dielectric measurements, we have studied the properties of x = 0.5 and 0.75, *i.e.* $[NH_3(CH_2)_2Cl]_2[CdCl_2Br_2]$ (**4**) and $[NH_3(CH_2)_2Cl]_2[CdClBr_3]$ (**5**), for systematically studying the variation of the phase transition temperature.

The preparation of crystals **4** and **5** was similar to that of **3**. For **4**, 2-chloroethanamine hydrochloride (10 mmol), 36% HCl (2 mL) and $CdCl_2{\cdot}4H_2O$ (5 mmol) were dissolved in deionized water (20 mL), and then 48% HBr (20 mmol) was added to the solution. As for **5**, to the aqueous solution (20 mL) of 2-chloroethanamine hydrochloride (10 mmol), 36% HCl (2 mL) and $CdCl_2{\cdot}4H_2O$ (5 mmol), 48% HBr (60 mmol) was added. A heating stage was required for the crystal growth (heating stage used to concentrate the solution), and after several days, the colourless flake single crystals of **4** and **5** were obtained. As illustrated in Fig. S7, DSC curves of **4** and **5** measured in a heating−cooling run display a pair of endothermic and exothermic peaks at 197.3/183.1 K and 235.4/218.3 K, respectively, signifying reversible first-order phase transitions. On the basis of DSC curves of **4** and **5**, the average entropy changes ΔS were estimated as 2.054 and 5.121 J (mol K)$^{-1}$, respectively. According to the Boltzmann equation $\Delta S = R\ln(N)$, the respective N values for **4** and **5** were calculated as 1.28 and 1.85, which are indicative of molecular dynamics. As shown in Fig. S8, the temperature-dependent dielectric constant (ε') of the polycrystalline samples of **4** and **5** measured at selected frequencies. For **4**, the dielectric anomaly appears at around 197 K, whereas for **5**, it is at around 227 K, in agreement with the phase transition temperatures determined by the DSC results. Besides, in the case of both **4** and **5**, at different frequencies, the temperature of dielectric anomaly shows almost no change, while the ε' value increases with the decrease of selected frequencies, indicating that there exists no dielectric relaxation.

The variation tendency of the phase transition temperatures of **4** and **5** is consistent with that of **1**, **2** and **3**. As depicted in the manuscript, by applying subtle anionic modifications on this series of layered organic-inorganic hybrid perovkite-type compounds, the phase transition temperature can be successfully tuned from low temperature to higher temperature and thus the practical value gets greatly improved. In regard to **1** (x = 1/4) and **3** (x = 1), with the increase of amount of Br, the closest distance between the anionic layers that provides room for the motions or reorientations of $[NH_3(CH_2)_2Cl]^+$ cations displays an obvious decrease. The smaller interlayer cavity makes the cationic motions restricted, so that **3** requires higher energy to pass through the barrier between two states and has a higher phase transition temperature. Combined with the research results of **4** (x = 0.5) and **5** (x = 0.75), when the amount of Br increases from 1/4 to 0.5, 0.75 and to 1, the phase transition temperature increases from 166.1/158 K to 197.3/183.1 K, 235.4/218.3 K and finally to 254.6/244.1 K.

Table S1 Crystal data and structure refinements for **1**, **2** and **3**.

Empirical formula	$(ClC_2H_4NH_3)_2$, $CdCl_3Br$ (**1**)	$(ClC_2H_4NH_3)_2$, $CdCl_3Br$ (**1**)	$(ClC_2H_4NH_3)_2$, $CdCl_4$ (**2**)	$(ClC_2H_4NH_3)_2$, $CdBr_4$ (**3**)
Formula weight	459.73	459.73	415.17	593.08
Crystal system	Orthorhombic	Orthorhombic	Orthorhombic	Orthorhombic
Space group	*Aba*2	*Aba*2	*Cmca*	*Aba*2
Temperature	293 K	143 K	293 K	293 K
a/Å	7.6707(10)	7.649(11)	7.5041(15)	7.9926(16)
b/Å	24.6215(19)	24.42(4)	24.658(5)	24.108(5)
c/Å	7.5742(10)	7.579(10)	7.4996(15)	7.9560(16)
α/deg	90	90	90	90
β/*deg*	90	90	90	90
γ/*deg*	90	90	90	90
Volume (Å^3), *Z*	1430.5(3), 4	1416(4), 4	1387.7(5), 4	1533.0(5), 4

F(000)	880.0	880.0	752.0	1096.0
Collected reflections	1623	1249	863	1360
Unique reflections	1089	1174	656	1358
Parameters refined	106	52	48	85
GOF	1.042	1.193	1.079	1.005
R_1/wR_2 [$I>2\sigma(I)$]	0.0554/ 0.1389	0.0826/ 0.2938	0.0740/ 0.2258	0.0755/ 0.2076

Table S2. Selected bond lengths [Å] and angles [°] for **1** at 143 K and 293 K.

143 K	Cd1—Br1	2.595 (4)	Cd1—Cl1^{iii}	2.643 (3)
	Cd1—Br1^{i}	2.595 (4)	Cd1—Cl1^{i}	2.771 (4)
	Cd1—Cl2	2.649 (6)	Cd1—Cl1	2.771 (4)
	Cd1—Cl2^{i}	2.649 (6)	Cl1—Cd1^{iv}	2.643 (3)
	Cd1—Cl1^{ii}	2.643 (3)	Cl2—Br1	0.570 (4)
	Br1—Cd1—Br1^{i}	172.81 (11)	Br1^{i}—Cd1—Cl1^{i}	92.25 (6)
	Br1—Cd1—Cl2	12.43 (9)	Cl2—Cd1—Cl1^{i}	81.00 (9)
	Br1^{i}—Cd1—Cl2	173.15 (10)	Cl2^{i}—Cd1—Cl1^{i}	88.60 (10)
	Br1—Cd1—Cl2^{i}	173.15 (10)	Cl1^{ii}—Cd1—Cl1^{i}	179.29 (10)
	Br1^{i}—Cd1—Cl2^{i}	12.43 (9)	Cl1^{iii}—Cd1—Cl1^{i}	88.86 (11)
	Cl2—Cd1—Cl2^{i}	165.07 (17)	Br1—Cd1—Cl1	92.25 (6)
	Br1—Cd1—Cl1^{ii}	87.57 (6)	Br1^{i}—Cd1—Cl1	92.76 (6)
	Br1^{i}—Cd1—Cl1^{ii}	87.37 (6)	Cl2—Cd1—Cl1	88.60 (10)
	Cl2—Cd1—Cl1^{ii}	99.37 (9)	Cl2^{i}—Cd1—Cl1	81.00 (9)
	Cl2^{i}—Cd1—Cl1^{ii}	91.15 (10)	Cl1^{ii}—Cd1—Cl1	88.86 (11)
	Br1—Cd1—Cl1^{iii}	87.37 (6)	Cl1^{iii}—Cd1—Cl1	179.29 (10)
	Br1^{i}—Cd1—Cl1^{iii}	87.56 (6)	Cl1^{i}—Cd1—Cl1	91.75 (15)
	Cl2—Cd1—Cl1^{iii}	91.15 (10)	Cd1^{iv}—Cl1—Cd1	167.91 (8)

	Cl2^{i}—Cd1—Cl1^{iii}	99.37 (9)	Br1—Cl2—Cd1	78.5 (4)
	Cl1^{ii}—Cd1—Cl1^{iii}	90.52 (15)	Cl2—Br1—Cd	89.1 (5)
	Br1—Cd1—Cl1^{i}	92.76 (6)		
293 K	Cd1—Br1	2.554 (3)	Cd1—Cl1^{ii}	2.720 (6)
	Cd1—Br1^{v}	2.554 (3)	Cd1—Cl1^{iii}	2.720 (6)
	Cd1—Cl2^{v}	2.714 (6)	Cl2—Br1^{v}	0.339 (13)
	Cd1—Cl2	2.714 (6)	Br1—Cl2^{v}	0.339 (13)
	Cd1—Cl1^{v}	2.705 (6)	Cl1—Cd1^{iv}	2.720 (6)
	Cd1—Cl1	2.705 (6)		
	Br1—Cd1—Br1^{v}	175.6 (3)	Br1^{v}—Cd1—Cl1^{vi}	93.58 (13)
	Br1—Cd1—Cl2^{v}	6.5 (3)	Cl2^{v}—Cd1—Cl1^{vi}	88.6 (2)
	Br1^{v}—Cd1—Cl2^{v}	176.12 (19)	Cl2—Cd1—Cl1^{vi}	87.2 (2)
	Br1—Cd1—Cl2	176.12 (19)	Cl1^{v}—Cd1—Cl1^{vi}	178.9 (3)
	Cl2^{v}—Cd1—Cl2	173.8 (6)	Br1—Cd1—Cl1^{iii}	93.58 (13)
	Br1—Cd1—Cl1^{v}	90.61 (11)	Br1^{v}—Cd1—Cl1^{iii}	89.48 (11)
	Br1^{v}—Cd1—Cl1^{v}	86.27 (13)	Cl2^{v}—Cd1—Cl1^{iii}	87.2 (2)
	Cl2^{v}—Cd1—Cl1^{v}	91.7 (2)	Cl2—Cd1—Cl1^{iii}	88.6 (2)
	Cl2—Cd1—Cl1^{v}	92.7 (2)	Cl1^{v}—Cd1—Cl1^{iii}	88.557 (13)
	Br1—Cd1—Cl1	86.27 (13)	Cl1—Cd1—Cl1^{iii}	178.9 (3)
	Br1^{v}—Cd1—Cl1	90.61 (11)	Cl1^{vi}—Cd1—Cl1^{iii}	92.6 (3)
	Cl2^{v}—Cd1—Cl1	92.7 (2)	Br1^{v}—Cl2—Cd1	58.7 (15)
	Cl2—Cd1—Cl1	91.7 (2)	Cl2^{v}—Br1—Cd1	114.8 (17)
	Cl1^{v}—Cd1—Cl1	90.3 (3)	Cd1—Cl1—Cd1^{iv}	166.99 (7)
	Br1—Cd1—Cl1^{vi}	89.48 (11)		

[a] Symmetry codes: (i) −*x*, −*y*+1, *z*; (ii) −*x*+1/2, *y*, *z*+1/2; (iii) *x*−1/2, −*y*+1, *z*+1/2; (iv) *x*+1/2, −*y*+1, *z*−1/2.(v) −*x*+1, −*y*+1, *z*; (vi) −*x*+3/2, *y*, *z*+1/2.

Table S3. Selected bond lengths [Å] and angles [°] for **2** at 293 K.

293 K	Cd1—Cl2	2.520 (4)	Cd1—Cl1^{iii}	2.6620 (5)
	Cd1—Cl2^{i}	2.521 (4)	Cd1—Cl1	2.6621 (5)
	Cd1—Cl1i	2.6620 (5)	Cl1—Cd1^{iv}	2.6621 (5)
	Cd1—Cl1^{ii}	2.6620 (5)		
	Cl2—Cd1—Cl2^{i}	180.0	Cl1^{i}—Cd1—Cl1^{iii}	89.62 (2)
	Cl2—Cd1—Cl1^{i}	89.92 (12)	Cl1^{ii}—Cd1—Cl1^{iii}	180.0
	Cl2^{i}—Cd1—Cl1^{i}	90.08 (12)	Cl2—Cd1—Cl1	90.08 (12)
	Cl2—Cd1—Cl1^{ii}	90.08 (12)	Cl2^{i}—Cd1—Cl1	89.92 (12)
	Cl2^{i}—Cd1—Cl1^{ii}	89.92 (12)	Cl1^{i}—Cd1—Cl1	180.0
	Cl1^{i}—Cd1—Cl1^{ii}	90.38 (2)	Cl1^{ii}—Cd1—Cl1	89.62 (2)
	Cl2—Cd1—Cl1^{iii}	89.92 (12)	Cl1^{iii}—Cd1—Cl1	90.38 (2)
	Cl2^{i}—Cd1—Cl1^{iii}	90.08 (12)	Cd1—Cl1—Cd1^{iv}	170.19 (19)

[b] Symmetry codes: (i) −x+3/2, y−1/2, −z+3/2; (ii) −x+3/2, y+1/2, −z+3/2; (iii) −x+1/2, y−1/2, −z+3/2; (iv) −x+1/2, y+1/2, −z+3/2.

Table S4. Selected bond lengths [Å] and angles [°] for **3** at 293 K**.**

293 K	Cd1—Br1^{i}	2.6337 (18)	Cd1—Br2^{ii}	2.886 (2)
	Cd1—Br1	2.6337 (18)	Cd1—Br2^{iii}	2.886 (2)
	Cd1—Br2	2.779 (2)	Br2—Cd1^{iv}	2.886 (2)
	Cd1—Br2^{i}	2.779 (2)		
	Br1^{i}—Cd1—Br1	175.7 (2)	Br2—Cd1—Br2^{ii}	177.38 (9)
	Br1^{i}—Cd1—Br2	88.59 (9)	Br2^{i}—Cd1—Br2^{ii}	89.301 (17)
	Br1—Cd1—Br2	88.35 (9)	Br1^{i}—Cd1—Br2^{iii}	92.04 (8)
	Br1^{i}—Cd1—Br2^{i}	88.35 (9)	Br1—Cd1—Br2^{iii}	90.88 (8)
	Br1—Cd1—Br2^{i}	88.59 (9)	Br2—Cd1—Br2^{iii}	89.301 (17)
	Br2—Cd1—Br2^{i}	88.12 (9)	Br2^{i}—Cd1—Br2^{iii}	177.38 (9)

$Br1^{i}$—Cd1—$Br2^{ii}$	90.88 (8)	$Br2^{ii}$—Cd1—$Br2^{iii}$	93.29 (9)
Br1—Cd1—$Br2^{ii}$	92.04 (8)	Cd1—Br2—$Cd1^{iv}$	169.09 (6)

[c] Symmetry codes: (i) −*x*, −*y*+1, *z*; (ii) *x*−1/2, −*y*+1, *z*−1/2; (iii) −*x*+1/2, *y*, *z*−1/2; (iv) *x*+1/2, −*y*+1, *z*+1/2.

Table S5. Temperature-dependent dielectric parameters: relaxation time (τ), distribution parameter (α), and dielectric increment (ε_0-ε_∞) for **1**.

T(K)	165	170	175	180
ε_∞	9.87	9.46	8.72	8.18
ε_0	33.58	35.55	45.52	52.64
$\tau\times10^{-6}$s	31.83	15.91	1.59	0.16
α	0.4276	0.2528	0.3737	0.3967